Numerical Analysis and Reinforcement Study of a Roadside Slope in Xinjiang

Hongwen Li [1, a], Bangxin Zhang [2, b], Lihong Wang [2, c], Dongming Peng [2, d], Guangqing Yang [2, e], Hongwei Li [2, f] and Chunyu Long [2, g]

[1] Guangdong Hualu Transportation Technology Co., Ltd., China;

[2] China Merchants Chongqing Communications Technology Research & Designinstitute Co.,Ltd., China.

[a] 381386707@qq.com, [b] 381804359@qq.com, [c] 373872225@qq.com, [d] 1258213871@qq.com, [e] 770293205@qq.com, [f] 120698102@qq.com, [g] 475642131@qq.com

Abstract. Road construction excavation on a road side slope stability constitutes a serious impact, in order to ensure the stability of the slope, the construction of finite element model analyzed the slope stress field, displacement field changes, determined that the slope stability coefficient of 1, does not meet the engineering requirements;Based on the numerical analysis and site investigation, two reinforcement schemes were determined: “Scheme 1: Anchor + Anti-slip Pile + Clearance; Scheme 2: Anchor + Anti-slip Pile + Interceptor Drainage”.The stability coefficient of the slope before reinforcement is increased by 38% in scheme 1, and 50% in scheme 2. Comprehensively comparing and analyzing the stress field and displacement field changes of the anchor and anti-slip piles as well as the stress field and displacement field of the slope body in the two schemes, and taking into consideration of the long-term stability of the slope and the economic cost, it is determined that scheme 1 is the final reinforcement scheme.

Keywords: slope; anti-slip pile; anchor; stability.

1. Introduction

Slope stability analysis and reinforcement management has been one of the hot issues in the field of geotechnical engineering, and has long been widely concerned by experts and scholars at home and abroad [1-3]. Wang Faling et al [4] studied the interaction between slope rock and anchors under the geological and structural conditions of down-gradient slopes, and established a mechanical model for anchor reinforcement of down-gradient slopes, and analyzed the accuracy of the mechanical model using numerical simulation; Sun Japing et al [5] constructed a calculation model of shear potential energy based on the principle of minimum potential energy to analyze the stability of slopes under the action of anchors; Yang Ying et al [6] through numerical simulation method, establish slope analysis model, discuss the reinforcement effect of anti-slip pile in the slope, analyze the deformation damage mechanism and overall stability of the slope; Zhu Yong et al [7] employed the strength reduction finite element method to investigate the influence of factors such as pile position and pile length on the reinforcement effect of anti-slide piles. Zhang Bangxin et al [8] based on finite element analysis means of comparative study of different reinforcement schemes on the slope stability impact; Rao Pingping et al [9] used the limit analysis upper limit method to analyze the damage mode of the slope and the stability of the slope after the anti-slip pile reinforcement by the parameter change of the influence of the law; Fu Qiang et al [10] carried out slope displacement, anti-slip pile top displacement and pile side pressure monitoring on the reinforced slope, and elaborated the dynamic stability of the slope after the slope reinforcement on the basis of the finite element mechanical analysis.

Anti-slip piles and anchors, as commonly used slope reinforcement measures, play an important role in improving the stability level of slopes. This paper takes a roadside slope in Xinjiang as the research object, constructs a slope finite element model, comparatively analyzes the stress field, displacement field, stability coefficient change and reinforcement effect of the two reinforcement

schemes, and determines the most suitable reinforcement scheme, and the research process has certain reference value for similar projects.

2. Slope profile

The slope is located in the proposed highway measured mileage of K227+596.32~K228+164.82, for the excavation slope, the design of the roadbed elevation of 1905.059m, the route to 250 ° orientation across the maximum height of the slope excavation 62.37m. is a low to medium hills terrain, topographic undulation is relatively large, the natural gradient of 20 ~ 28 °, locally steep.Slope without faults, folds and other geological formations, stratigraphic lithology of a single composition, the distribution of continuous, for the gravel soil slopes; the section of the overall trend of the topography of the high south and low north, the road graben area has no surface water distribution, the survey period of the boreholes did not see groundwater. After the field investigation and expert analysis to determine the potential main sliding surface of the slope as shown in Fig. 1, in order to ensure the safety of road construction at the foot of the slope, the stability analysis of the slope.

Fig. 1 Potential main sliding surface of the slope

3. Numerical analysis

The geological structure of the potential main sliding surface of the slope was determined by the field investigation as shown in Fig. 2, and the physico-mechanical parameters of the slope geotechnical body were obtained from the indoor and outdoor experiments as shown in Table 1.

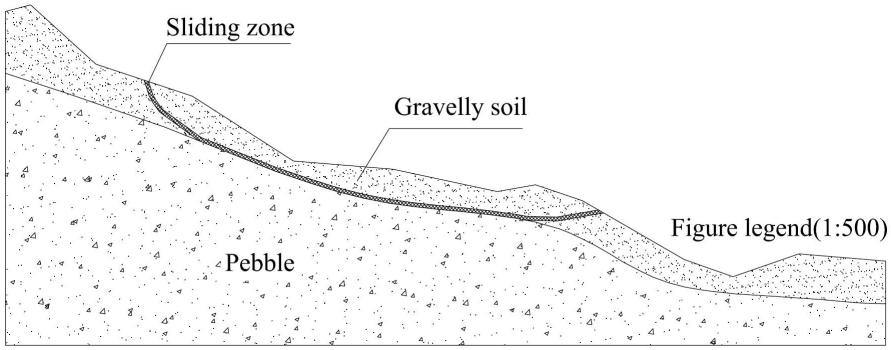

Fig. 2 Geologic configuration of the potential main sliding surface

Table. 1 Physical and mechanical parameters

Form	Severe/(kN.m^{-3})	Cohesive force/kPa	Friction angle/(°)	Modulus of elasticity/MPa	Poisson's ratio
Sliding zone	18	21.5	16	14	0.3
Gravelly soil	20	16	20	20	0.32
Pebble	24	5	42	200	0.35
Pile	24	-	-	30000	0.2
Anchor rods	-	-	-	200000	0.35

The finite element model of the slope is constructed as shown in Fig. 3, with fixed constraints applied to the bottom and both sides of the model, and meshed using CPE4 cell type.

Based on the slope finite element model for the slope, the stress field, displacement field and stability coefficient changes, the average stress cloud of the slope is obtained as shown in Fig. 4, and the displacement cloud is shown in Fig. 5.

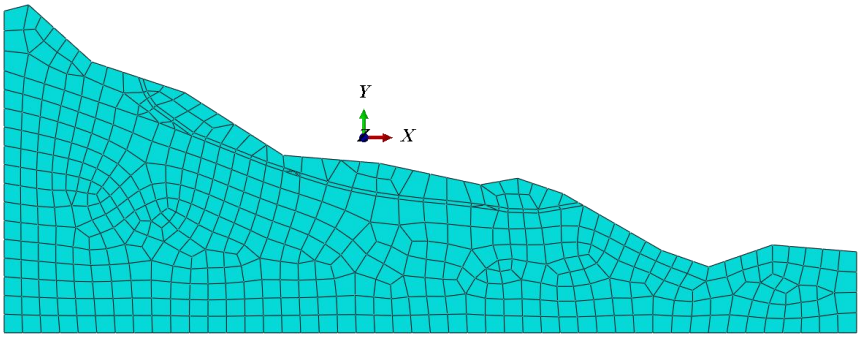

Fig. 3 Finite element model

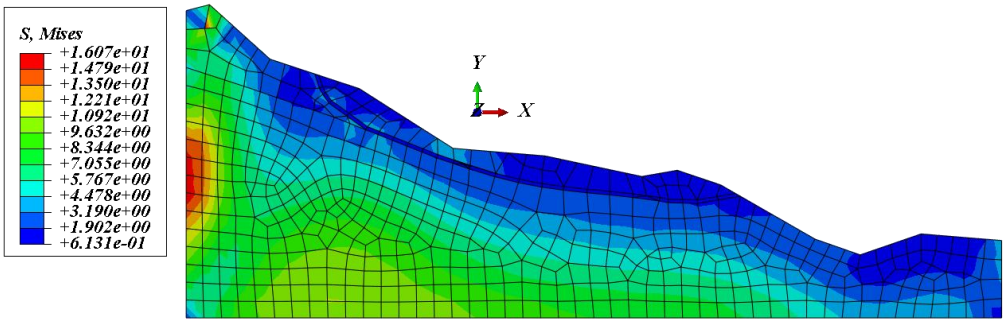

Fig. 4 Stress cloud diagram

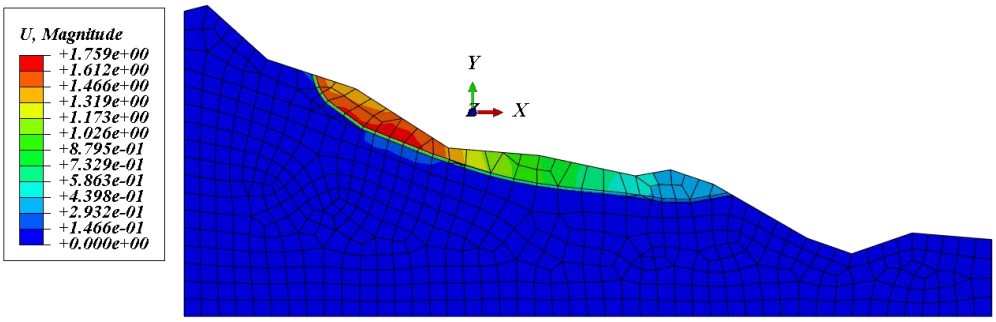

Fig. 5 Displacement cloud map

From Fig. 4, it can be seen that: the average stress of the surface gravel soil is small, and the average stress of the inner pebble layer is large; the maximum value of the average stress is 16.07kPa, which is located in the pebble layer against the back edge of the slope body, and the minimum value of the average stress is 0.6kPa. From Fig. 5, it can be seen that: the area where the change of the displacement occurs is centered on the sliding zone and the gravel soil overlaying layer above it, and the maximum value of the displacement is 175.9mm, while the lower pebble layer has not been displaced. Pebble layer was not displaced.

Taking the starting point of the area where the displacement change occurs as the study point, and taking the inflection point of the displacement value appearing as the slope stability evaluation criterion, the stability coefficient change curve of the potential main sliding surface is obtained as shown in Fig. 6.

It can be seen from Fig. 6: the stability coefficient changes abruptly when it reaches 1. According to the displacement change judgment standard of slope stability evaluation, the stability coefficient of the potential main sliding surface is determined to be 1, and the relevant standards require that the stability coefficient of this kind of slope under natural working condition ranges from 1.2 to 1.3, indicating that the current slope stability level does not meet the engineering requirements, and there exists the risk of destabilization, which needs to be carried out by reinforcing measures. Slope management.

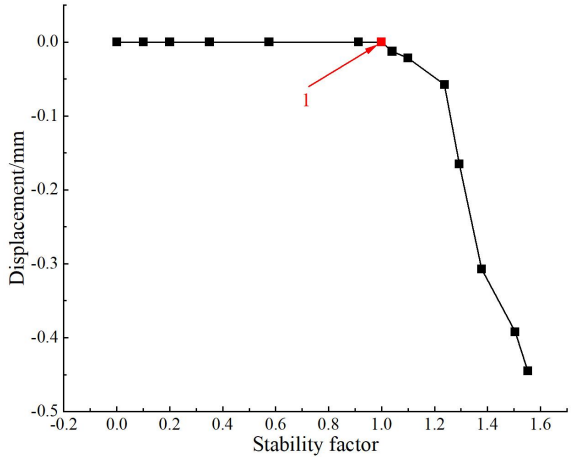

Fig. 6 Stability coefficient variation curve

4. Reinforcement management

Combined with the site investigation and finite element numerical analysis results, Scheme 1: anchor + anti-slip piles + clearing, set square row of piles, cross-section of 2 × 3m, pile spacing of 2m, pile length of 18m, embedded section of 14m; anchor deployment in the middle and upper part of the slope layout, spacing of 2m, the length of 11.5m, inclination of 60° and 75° , and to remove the foot of the slope of the piled up soil, the specific layout of the schematic diagram shown in Fig. 7. Scheme 2: Anchor + anti-slip piles + intercepting and draining, set up 3 rows of square anti-slip piles, the cross section are 2×3m, the pile spacing are 2m, the embedded section of 22m long piles is 16m, the embedded section of 20m long piles is 15m, the embedded section of 18m long piles is 14m, and build slurry masonry schist intercepting ditch in the back edge of the slope, and the specific laying schematic diagram is shown in Fig. 8.

The finite element models of the reinforcement scheme were constructed as shown in Fig. 9 and 10, respectively, with fixed constraints in the horizontal and vertical directions applied to the bottom and both sides of the models, and a nonlinear analysis was used, in which the slope was of the CPE4 cell type, the anti-slip piles were of the B21 cell type, and the anchors were of the T2D2 cell type.

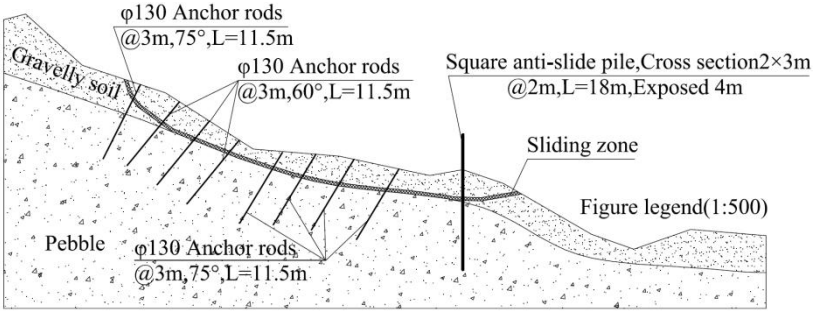

Fig. 7 Schematic layout of scheme 1

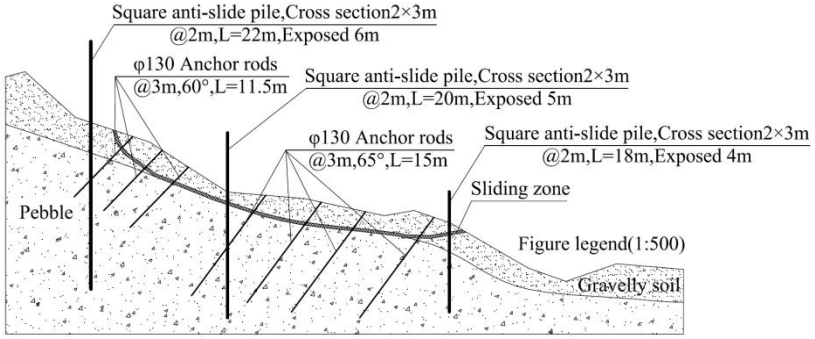

Fig. 8 Schematic layout of scheme 2

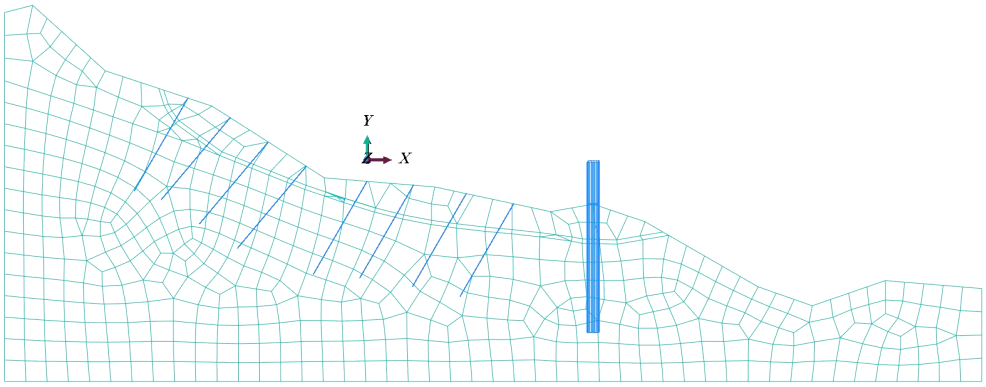

Fig. 9 Scheme 1 finite element model

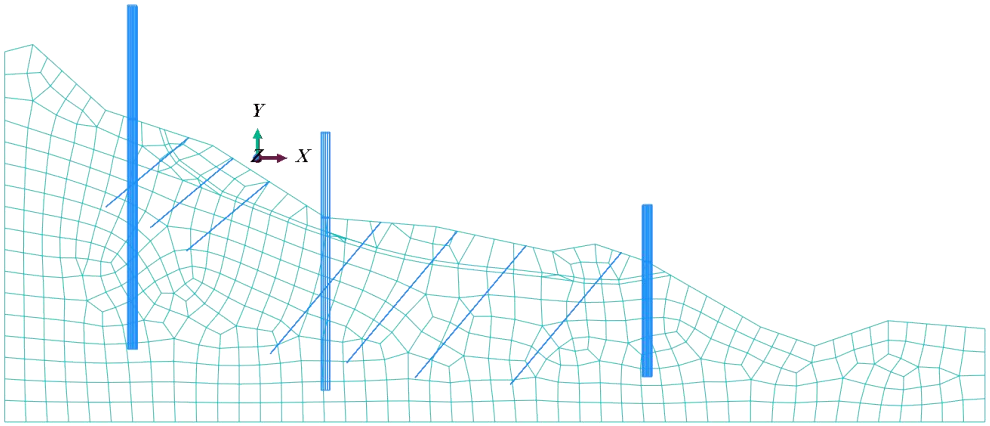

Fig. 10 Scheme 2 finite element model

Numerical analyses yielded average stress clouds for the two reinforcement schemes as shown in Fig. 11 and 12, respectively; displacement clouds are shown in Fig. 13 and 14.

From Fig. 11 to Fig. 14, it can be seen that: the maximum average stress of scheme 1 is 14.72× 103kPa, and it is mainly concentrated on the anchor rods, and the overall average stress of the skid-resistant piles and the slope body is small, and the maximum average stress of scheme 2 is 25.94 × 103kPa, which is mainly concentrated on the anchor rods, and it is increased by 76.22% compared with that of scheme 1, and the overall average stress of the skid-resistant piles and the slope body is small;The displacement deformation of scheme 1 is mainly concentrated in the anti-slip piles, around the anchors and the potential sliding zone and the gravel soil cover above it, with a maximum displacement of 37.2 mm, while the displacement deformation of scheme 2 is mainly concentrated in the anti-slip piles, around the anchors, part of the inner area of the slope, the potential sliding zone and the gravel soil cover above it, with a maximum displacement of 52.56 mm, which is 41.29% higher compared to that of scheme 1. The rest of the region displacement and deformation is smaller.

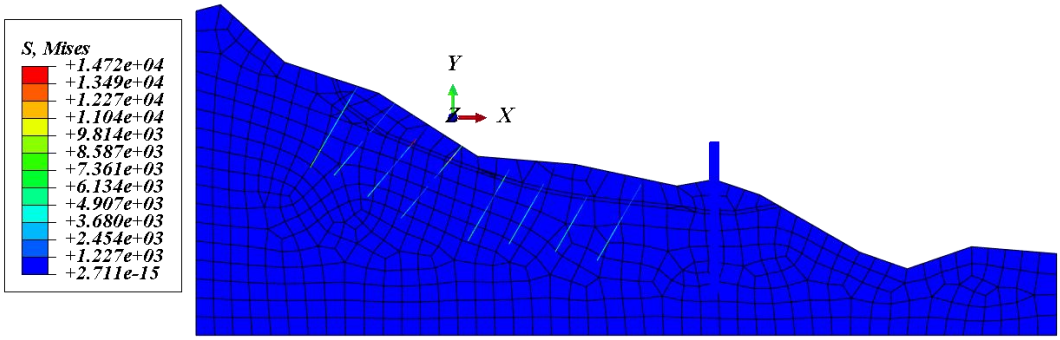

Fig. 11 Average stress cloud for scheme 1

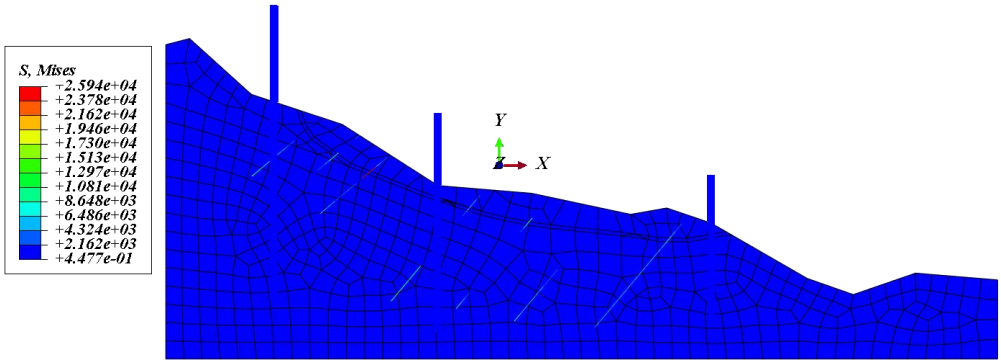

Fig. 12 Average stress cloud for scheme 2

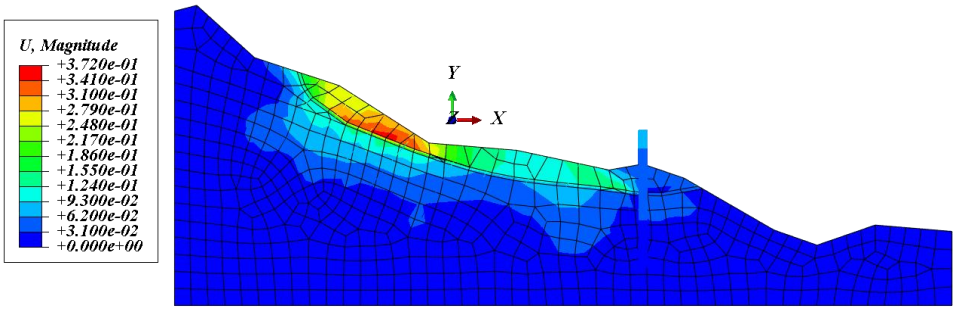

Fig. 13 Scheme 1 displacement cloud

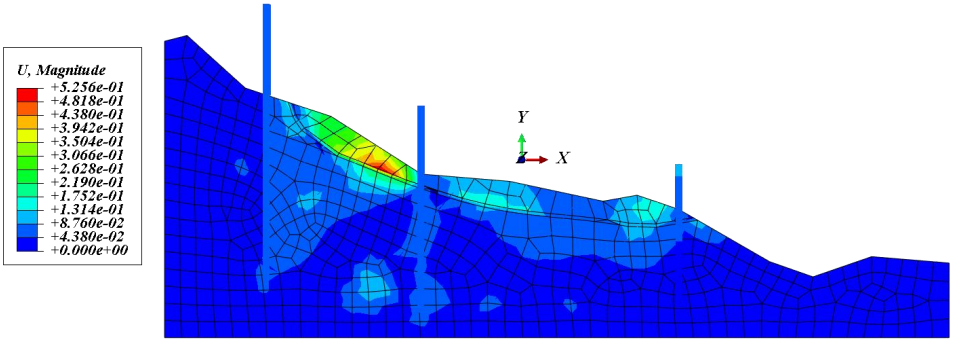

Fig. 14 Scheme 2 displacement cloud

Taking the starting point of the potential sliding zone as the final study point and the inflection point of the slope displacement and deformation amount as the judgment criterion of slope instability, the change curves of stability coefficients of the two reinforcement schemes are obtained as shown in Fig. 15.

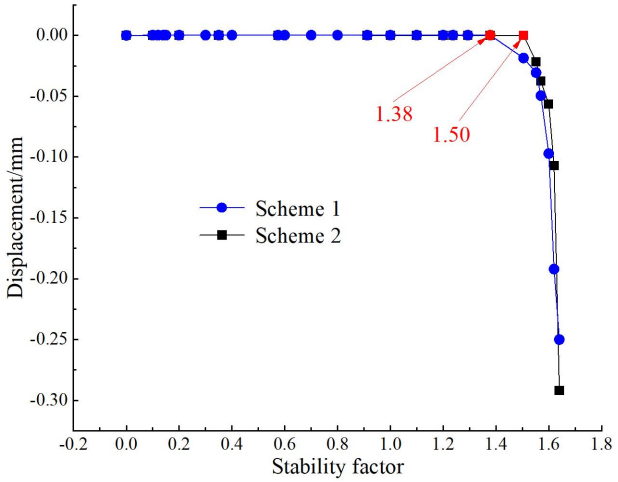

Fig. 15 Stability coefficient variation curves for the reinforcement scheme

As can be seen from the figure: the slope stability coefficient corresponding to the reinforcement scheme 1 is 1.38, which is 38% higher than that of the unreinforced condition, and the slope

stability coefficient corresponding to the reinforcement scheme 2 is 1.50, which is 50% higher than that of the unreinforced condition, indicating that the two reinforcement plans can effectively improve the stability of the slopes while meeting the requirements of the relevant standards and specifications. level.

The reinforcement scheme used in Scheme 1 is simpler and less difficult to construct compared to Scheme 2. Considering the economic cost and reinforcement effect of the two reinforcement schemes, it is determined that Scheme 1 is adopted as the final reinforcement scheme.

5. Summary

1) The stability coefficient of the slope before reinforcement is 1, which does not meet the specification requirements, and the surface slope is in an unstable state.

2) Scheme 1 corresponds to a slope stability coefficient of 1.38, which is 38% higher than that before reinforcement; Scheme 2 corresponds to a slope stability coefficient of 1.50, which is 50% higher than that before reinforcement, indicating that the two reinforcement schemes are feasible, and both of them effectively improve the stability level of slopes.

3) Considering the economic cost and reinforcement effect of the two reinforcement schemes, scheme 1 is identified as the final reinforcement scheme.

Acknowledgments

This work was financially supported by National Key R&D Project (2022YFC3002603), Chongqing Natural Science Foundation Upper-level Project (CSTB2023NSCQ-MSX0878), General Research and Development Science and Technology Project of Guangdong Provincial Communications Group Co., Ltd. (JT2024YB06), Major Science and Technology Special Project/Key R&D Task Special Project of the Autonomous Region (2022B03033-2).

References

[1] Xu Shumei, Xiao Lin, Li Chengcheng, et al. Status review on two kinds of typical geological hazard zoning techniques in China. Journal of Natural Disasters, 2017, 26(2): 22-31.

[2] Zhang Jiangwei, Li Xiaojun, Chi Mingjie, et al. Analysis of formation mechanism and characteristics of landslide disasters. Journal of Natural Disasters, 2015, 24(6): 42-49.

[3] Lin Shan, Guo Yukui, Sun Guanhua, et al. Imaginary unit strength discount method for slope stability analysis. Journal of Rock Mechanics and Engineering, 2019, 38(S2): 3429-3438.

[4] Wang Faling, Liu Caihua, Gong Zhe． Research on anchor support mechanism of smooth rocky slopes. Journal of Rock Mechanics and Engineering, 2014, 33(7): 1465-1470.

[5] Sun Jiaping, Gu Houyu, Hu Guobao, et al. Study on improved minimum potential energy method in slope stability analysis under the action of anchor bolt. Rock and Soil Mechanics, 2017, 38(S1): 291-298.

[6] Yang Ying, Xu Nuwen, Li Tao, et al. Stability analysis of the left bank slope of Baihetan Hydropower Station based on RFPA~(3D)and microseismic monitoring. Rock and Soil Mechanics, 2008, 39(6): 2193-2202.

[7] Zhu Yong, Zhu Honghu, Zhang Wei, et al. Parametric Analysis of Factors Influencing the Stability of Slopes Reinforced with Anti-slide Piles. Journal of Engineering Geology, 2017, 25(3): 833-840.

[8] Zhang Bangxin, Jia Jianqing, Liu Zhongshuai, et al. Stability analysis of Xiafen slope and its management measures. Journal of Lanzhou Jiaotong University, 2023, 42(1): 9-15.

[9] Rao Pingping, Zhao Linxue, Liu Ying, et al. Analysis of three-dimensional limit and upper limit expansion of slope stability strengthened by anti-slide piles. Advanced Engineering Sciences, 2008, 50(6): 184-192.

[10] Fu Qiang, Sun Feifei, Tang Chengtie, et al. Antisliding effect of double-row miniature anti-sliding pile. Journal of Central South University(Science and Technology), 2013, 44(4): 1596-1602.